595

Fabrication and optical properties of lead-germanate glasses and a new class of optical fibers doped with Tm^{3+}

J. Wang
Optoelectronics Research Centre, The University, Southampton SO9 5NH, United Kingdom

J. R. Lincoln
Department of Physics, The University, Southampton SO9 5NH, United Kingdom

W. S. Brocklesby
Optoelectronics Research Centre and Department of Physics, The University, Southampton SO9 5NH, United Kingdom

R. S. Deol and C. J. Mackechnie
Optoelectronics Research Centre, The University, Southampton SO9 5NH, United Kingdom

A. Pearson
Department of Physics, The University, Southampton SO9 5NH, United Kingdom

A. C. Tropper, D. C. Hanna, and D. N. Payne
Optoelectronics Research Centre, The University, Southampton SO9 5NH, United Kingdom

(Received 21 September 1992; accepted for publication 15 March 1993)

In this article we present a study of a new class of optical fibers based on lead germanate glass. The maximum vibrational frequency of this glass is intermediate between silica and zirconium barium lanthanum aluminum fluoride glass, causing a beneficial change in nonradiative decay and therefore quantum efficiency for particular laser transitions. Fabrication of high-strength, low-loss fibers of this glass has been acheived by modification of the composition to produce optimal physical properties for fiber drawing, while retaining the useful vibrational properties of the original $PbGeO_2$ glass. Measurements of both the thermal and optical properties are described. The fibers produced are ideal for many applications in fiber devices.

I. INTRODUCTION

Rare-earth doped optical fibers have received considerable attention in recent years due to the enhanced performance that optically pumped fiber devices can give over bulk glass devices. The major advantage of fiber technology is the guiding, and therefore confinement of light, which can increase the interaction volume of the pump light with the active medium while maintaining high light intensities.[1] The principal limiting factor on the number of devices which have been demonstrated in optical fiber structures has been the very small number of glasses that have been fabricated into the low-loss optical fiber necessary for efficient device performance. For many years low-loss fiber fabrication has been confined to silica or modified silica glasses, although in the last 2–3 years fluoride-based zirconium barium lanthanum aluminum (ZBLAN) glass fibers have also become available. We see it as absolutely essential that the range of rare-earth doped glasses that can be made into fiber structures is extended, particularly into lower vibrational-energy glasses combining possibly the best properties of both silica (low loss, high strength, etc.) and fluoride-based glasses (low nonradiative relaxation rate, etc.).

In this article, we report the preparation and characterization of Tm^{3+}-doped lead-germanate based glasses and fibers. Fabrication of a lead-germanate glass suitable for fiber-optic applications is successfully achieved by optimizing the glass composition using the Levin-Block concept developed in late 1960's.[2–4] The optimized lead-germanate glass shows a remarkable thermal-stability characteristic, exhibiting no devitrification phenomenon throughout the entire temperature range from the glass transition temperature T_g to the melting temperature T_m. Particular silicate glasses which are both thermally and optically compatible with the optimized lead-germanate core glass are identified as suitable cladding materials. These lead to the realization of a new class of rare-earth doped, low loss, high strength as well as low cost, multicomponent-glass optical fibers suitable for fiber device applications, by a simple, flexible conventional rod-in-tube technique.

Raman spectra of a range of lead-germanate based glasses confirm that the maximum vibrational energy of these glasses is intermediate between those of silica and fluoride-based glasses. The smaller frequency shift of the maximum vibrational-energy peaks in the Raman spectra of lead germanates compared to that of pure germania glass is examined and interpreted with respect to the role of Pb^{2+} in the glasses.

Absorption and emission spectra, together with electronic level decay times for Tm^{3+}-doped lead-germanate provide an extensive characterization of the optical properties of this rare-earth ion in the lead-germanate host. The reduced maximum vibrational energy of lead-germanates ($890\ cm^{-1}$) over that of silicates ($1150\ cm^{-1}$) produces a substantial gain in extending the metastable level lifetimes in Tm^{3+}, as expected with the prediction from the multiphonon decay mechanism. On the other hand, the main-

 0021-8979/93/128066-10$06.00

tenance of the maximum vibrational energy above that found in fluoride-based ZBLAN (580 cm^{-1}) enables multiphonon emission to be utilized with high efficiency in populating the upper level of Tm^{3+} $^3H_4 \rightarrow {}^3H_6$ the transition. This enhances the performance of lasing this $^3H_4 \rightarrow {}^3H_6$ transition at around 2 μm with a laser diode compatible pumping scheme[5] by exciting the Tm^{3+} $^3F_4$ level at a wavelength around 790 nm. Improvements in the 2 μm fiber laser performance in a lead-germanate fiber host compared to those in silica and fluoride-based ZBLAN, glass fiber hosts are noted and have been reported earlier.[6] Comparison of the optical properties of Tm^{3+}-doped germania and various modified lead germanates confirms the dominant role of Pb^{2+} in the latter in influencing the glass structure and properties. The variation in the lifetimes of Tm^{3+} electronic levels between different bulk lead germanates and lead-germanate fiber is also addressed.

II. EXPERIMENTAL TECHNIQUES

A. Glass preparation

Glasses were prepared from anhydrous oxide powders for Ge, Al, Zn, Pb, and Tm, and anhydrous carbonate powders for Ba, Ca, and K. All chemicals were of common analytical grade except for GeO_2 which was of electronic grade (99.999% purity, Aldrich Chemical Company), and Tm_2O_3 which was of 99.9% purity (Aldrich Chemical Company). Glass batches, in quantities of 150–200 g of powder, were mixed for at least half an hour in a cleaned glass container mounted on a rotating lathe. Batches were then melted in a platinum crucible placed in an electrically heated furnace, containing an air atmosphere, at temperatures between 1000 and 1250 °C. The melts were kept well stirred with a silica rod to achieve homogeneous mixing, and later refined to remove bubbles. The refined glass melts were removed from the furnace at 1150 °C and cast into a prewarmed stainless-steel mould before being annealed in a muffle furnace at around 500 °C. All glasses contained 0.5 wt. % Tm_2O_3 as an active dopant. A series of smaller undoped samples, prepared from 20 g of powdered constituents were also made for the thermal treatment tests, using a similar temperature arrangement to the larger samples. Homogeneity was achieved in the smaller samples by shaking, rather than stirring, the melts in the crucible at 1200 °C.

B. Thermal analysis

Thermal analysis of the glasses was carried out on a commercial Netzsch 404 type differential scanning calorimeter (DSC). Powdered samples, typically about 50 mg, were heated at a rate of 20 °C per minute, from room temperature to 1100 °C in an air atmosphere. The crucibles used were matched pairs made of alumina, and the temperature precision was ±0.1 °C. The thermal stability of the bulk lead-germanate glasses was also tested by placing samples in a muffle furnace heated to the likely fiber pulling temperatures, around 750 °C, and then holding the samples at that temperature in the furnace for half an hour to assess their crystallization tendencies.

C. Spectroscopy

Raman spectra were recorded using a commercial triple grating spectrometer equipped with a nitrogen cooled charge coupled device (CCD) detector. Bulk glass samples were excited with an argon-ion laser at either 514.5 or 488 nm and the Raman signal recorded in a 180° backscattering geometry. No polarization selection was used in detection. Absorption spectra were recorded from polished bulk glass samples on a white light spectrophotometer (Perkin-Elmer Lambda 9) with automatic correction for detector response.

Visible fluorescence spectra and decay times were measured by exciting samples with either an argon-ion laser or an argon-pumped Pyridine 2 dye laser. The excitation beam was chopped with an acousto-optic modulator and the pump light focused onto the bulk sample or into the core of the optical fiber. Fluorescence was monitored from light scattered out of the side of fibers, or from close to the surface of bulk samples. Emission spectra were recorded on a 1 m spectrometer, equipped with a photon counting GaAs photomultiplier tube. Lifetimes, of visible fluorescence, were taken using the same apparatus and using the photon counter as a box car averager. Infrared fluorescence spectra were recorded using a scanning 0.3 m spectrometer and PbS photodiode detector. Infrared lifetimes were recorded using a nitrogen cooled InAs photodetector and germanium filters to block the visible light. Decay times were derived by fitting a single exponential decay function to the observed fluorescence decay using a statistically weighted nonlinear least-squares fit routine.

III. FABRICATION OF A LEAD-GERMANATE GLASS SUITABLE FOR FIBER-OPTIC APPLICATIONS

A. Initial trials

Glasses based on germanium dioxide have long been known to have better infrared (IR) transmission than glasses based on silicon dioxide, extending in some cases up to 5.5 μm.[7] This extended IR transmission is due to the larger size and the heavier mass of germanium when compared to silicon. The Ge^{4+} is therefore more weakly bonded to the surrounding O^{2-} ions and the associated bonds have lower vibrational frequencies and energies than similar Si—O bonds. The weaker bonding also means glasses based on GeO_2 have smaller stable glass formation ranges than glasses based on SiO_2.[8] The manufacture of multicomponent germanate glasses, without devitrification, is therefore harder than similar silica based systems, and may require more rapid quenching rates. Pure GeO_2 glass and germania-rich glasses are also known to have a tendency to react with atmospheric moisture,[9] again undesirable for high-grade optical fibers.

It has been previously reported that a series of lead-germanate based ternary glass systems have relatively large glass forming regions, compared to other germanate systems, while maintaining high infrared transmission.[10] Among these, a specific glass of the composition $63GeO_2$-27PbO-10CaO (in mole percentage) was also noted to have inherently less OH^- contamination. Therefore, a lead

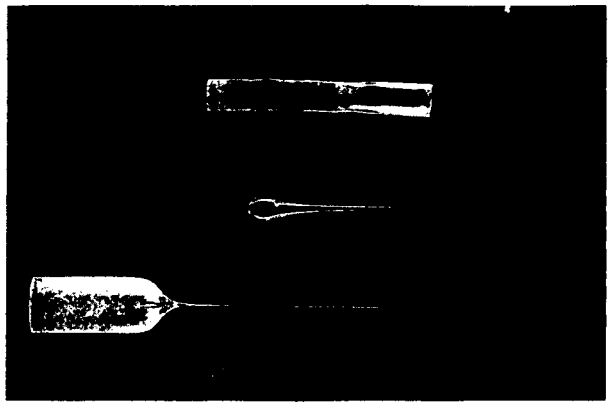

FIG. 1. (a) Glass rod of composition $63GeO_2$-27PbO-10CaO, crystallized in fiber-drawing furnace at 700 °C for 30 min. (b) Successfully caned glass rod of composition in system GeO_2-PbO-BaO-ZnO-K_2O, showing no crystallization at 700 °C. (c) The rod-in-tube preform and the fiber with core of composition in the GeO_2-PbO-BaO-ZnO-K_2O system, and cladding of Schott SF56.

germanate glass with initial composition $63GeO_2$-27PbO-10CaO was fabricated at 1050 °C in air, to be evaluated for fiber fabrication. The resulting glass, made from this composition, was found to be stable by the conventional casting procedure, and no devitrification either on surface or in volume form was observed for the bulk materials. The fiber pulling temperature, corresponding to viscosity η of about 10^5 P, for this glass was estimated as 50–100 °C above T_s, where $\eta = 10^{7.6}$ P. The value of T_s was obtained from the two-third rule,[11] an empirical relationship between T_g and T_s, resulting in a fiber pulling temperature range of 700–750 °C. However, as shown in Fig. 1(a), devitrification occurred in the hot zone of the fiber pulling furnace when attempting to pull this glass into a fiber at temperatures around 700–750 °C. The DSC measurement of this initial glass, presented in Fig. 2, clearly shows two exothermic peaks at around 710 and 750 °C respectively, indicating strong crystallization at these temperatures. The severe crystallization of this $63GeO_2$-27PbO-10CaO glass in the fiber pulling temperature range made this composition useless for its fiber optic applications.

In order to further stabilize the glass up to 10 mol % aluminium oxide, Al_2O_3, was added to the initial glass

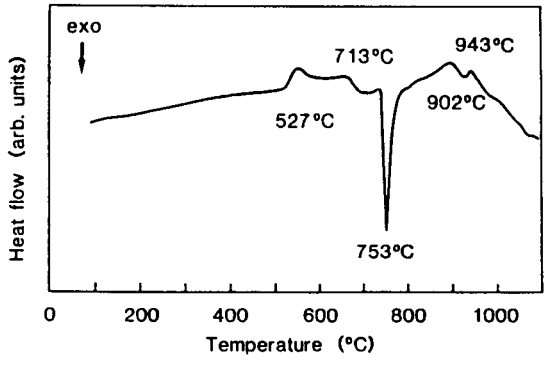

FIG. 2. DSC curve of glass with composition $63GeO_2$-27PbO-10CaO.

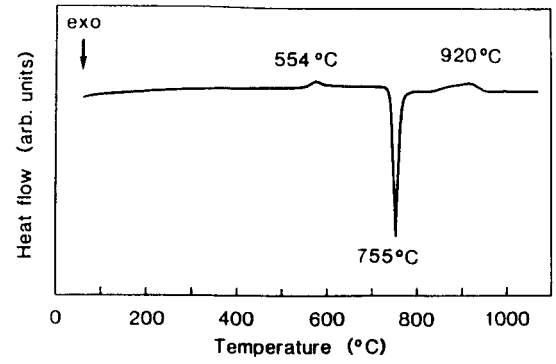

FIG. 3. DSC curve of glass with composition $63GeO_2$-27PbO-10CaO-$5Al_2O_3$.

composition, since it is known[12] that alumina is effective in stabilizing some silicate glass melts by acting as additional linkages for the three-dimensional glass framework that is partially broken by the glass modifiers. Following preparation of a series of modified lead-germanate glasses with compositions

$$63GeO_2\text{-}27PbO\text{-}10CaO\text{-}xAl_2O_3, \quad x=1,\ 2,\ 5,\ \text{and}\ 10$$

at 1150–1250 °C, thermal tests of the glasses in a muffle furnace at 750 °C for 30 min showed that all samples devitrified. The DSC measurements were also conducted and the results for the sample $x=5$ is shown in Fig. 3. It can be seen from Fig. 3 that the exothermic peak indicating crystallization at 710 °C that was observed in the original $63GeO_2$-27PbO-10CaO glass (Fig. 2) has been eliminated on the addition of alumina. However, the more severe exotherm-crystallization peak at 750 °C was still present (Fig. 3) despite the addition of alumina. The substitution of CaO by BaO was also made in above system. However, thermal treatment tests at 750 °C in a muffle furnace showed similar devitrification features to the CaO containing glasses. It was therefore concluded that alumina is not a sufficiently efficient intermediate component in the lead-germanate glass system to provide the high-temperature glass stability which is crucial for fiber fabrication. Hence, another, more effective, intermediate component must be established to give high-temperature stability to the lead-germanate glasses.

B. The Levin-Block concept

Levin and Block, in the 1960's (Refs. 2–4) have systematically studied the immiscibility phenomenon in oxide glass systems by applying the principles of crystal chemistry. They concluded that the occurrence of immiscibility in a glass was purely governed by the bond strengths of the modifying and the intermediate cationic ions involved in the glass. To quantify the bond strength, they used the ionic field strength (IFS) defined as

$$\text{IFS}=\frac{Z}{(R^{+}+1.40)^2}, \tag{1}$$

where Z is the charge on the cation and the $(R^+ + 1.40)$ term is the interatomic separation, taken as the sum of the cationic radius and the oxygen ionic radius. It was suggested that the extra phases would not occur if the modifying or intermediate cation-oxygen field strengths were either too strong or too weak relative to the corresponding strength of glass former in the system. Quantitatively, a system would remain in a single phase if the difference in ionic field strengths between the glass former and the modifier (ΔIFS) was greater than 0.8 or less than 0.06.[4,13] For the case of an intermediate component, the actual figures were not given, however the similar principle should be followed. We believe that the Levin–Block principle can also be applied to the crystallization, as well as the glass phase separation, since the occurrence of extra phases either in glass or in crystal form is a matter of where the glass composition is situated in the specific phase diagram. Although the Levin–Block concept has been criticized for its ignoring the influence of temperature,[14] it has been found appropriate for most of the oxide systems, including the germanate systems;[4,13] it should therefore provide a general basic guidance for the optimization of glass compositions.

C. Optimizing the composition suitable for fiber fabrication

It is known that the basic germanate glass structural unit, consisting of germanium-oxygen GeO_4 tetrahedra, has a larger volume than the SiO_4 tetrahedra found in silicate glasses, with a Ge—O bond distance of 1.74 Å in pure GeO_2 glass in contrast to a Si—O bond distance of 1.60 Å in silica.[15] The corresponding ionic field strengths (IFS) for Ge—O and Si—O bonds are 1.074 and 1.208, respectively.[13] According to the Levin–Block concept, in order to maintain the difference of IFS between the glass former and the modifier within the same required limits, the modifiers required by germanate glass should have lower IFS values than those required by silicate glass. From Eq. (1), this means that a larger modifying ion size is demanded for the stable formation of germanate glasses, compared to the formation of silicate glass, if the same charged ions are used. A similar trend should also be followed by the intermediate ions.

For the germanate glasses we utilized ZnO as an intermediate element instead of Al_2O_3, since Zn^{2+} has an ionic radius, $R_{Zn^{2+}}$, of 0.74 Å,[13] much larger than the ionic radius of Al^{3+}, $R_{Al^{3+}} = 0.51$ Å. More importantly, it can be noted that the Zn—O bond possesses a ΔIFS of about 0.6 relative to Ge—O compared with only 0.25 for Al—O relative to Ge—O. The latter can be contrasted to the Al—O bond relative to Si—O, which has a ΔIFS of about 0.4.[13] We believe that it is the insufficient difference in IFS for alumina in germanate that accounts for its weakness as an effective intermediate component. For the modifier component, according to the Levin–Block concept, barium oxide, BaO, was found to be more suitable than CaO. Barium oxide, $R_{Ba^{2+}} = 1.34$ Å, has a ΔIFS value of 0.81 relative to Ge—O, just above the critical value of 0.8, while calcium oxide CaO, $R_{Ca^{2+}} = 0.99$ Å, has a ΔIFS value of 0.72 relative to Ge—O less than the required 0.8. To further ensure ZnO acted as the intermediate component, potassium oxide K_2O ($R_{K^{1+}} = 1.33$ Å, ΔIFS = 0.94 > 0.8 relative to Ge—O) was also added to the composition as a modifier providing extra free O^{-2} ions required for the possible formation of ZnO_4 tetrahedral units in the glass network.[16]

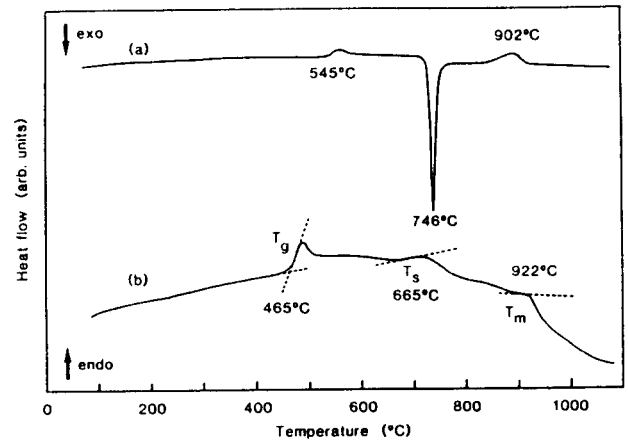

FIG. 4. DSC curves of two glasses in the systems (a) GeO_2-PbO-CaO-ZnO-K_2O and (b) GeO_2-PbO-BaO-ZnO-K_2O.

In order to make a proper estimation of the amount of each ingredient in the glass, the following two points were considered. First, the ratio of GeO_2/PbO was required to be near 3, because the phase diagram of the GeO_2-PbO binary system exhibits crystal compounds at GeO_2/PbO ratios of both 2 and 4.[17] For a stable glass formation, it was desirable to be as far from these points as possible. Secondly, the ratio of $R_2O(RO)$/ZnO need to be much grater than unity, to ensure the formation of ZnO_4.[16] Consequently, the following glass compositions were designed:

(a) $55GeO_2$-20PbO-10CaO-10ZnO-$5K_2O$,

(b) $55GeO_2$-20PbO-10BaO-10ZnO-$5K_2O$.

Composition (a), with CaO still a modifier, was fabricated to test the Levin–Block concept. The thermal treatment tests carried out at 750 °C in a muffle furnace for the two glasses prepared from the above compositions showed that as anticipated glass (a) crystallized, but glass (b) exhibited no crystallization. The DSC measurements of the two glasses are shown in the upper and lower halves of Fig. 4. For glass (a) a similar crystallization, exotherm, peak can be seen similar to those exhibited by the previous glass samples although it appears at the slightly lower temperature of 746 °C, instead of 755 °C. From the lower part of Fig. 4 it can be seen that glass (b) shows no exotherm peaks, and therefore no crystallization, over the entire temperature range from T_g to T_m. Glass of composition (b), now abbreviated to GPBZK, is therefore extremely stable and was chosen for fiber production purposes.

Further examination of the DSC curve of glass (b), shown in the lower part of Fig. 4, gave values for T_g of about 465 °C, T_s of about 665 °C, and T_m of about 922 °C for this glass. These were determined by the intersects be-

tween the base line and the starting edges of the respective small endothermic humps in the DSC curve,[18] as shown in Fig. 4. Caning of glass rod of composition (b), in a fiber pulling furnace, was successfully performed at about 700 °C, as shown in Fig. 1(b).

The above results illustrate the usefulness of the Levin–Block concept in optimizing the glass compositions. To our knowledge, this has been the first time the Levin–Block concept has been utilised in this way for the optimization of compositions for stable glass formation.

IV. CLADDING GLASSES AND FIBER MANUFACTURING

A. Cladding glasses

In order to fabricate our optimized lead germanate glass into an optical fiber structure, a suitable cladding glass had to be found with compatible optical, thermal, and chemical properties to our core glass. The most obvious cladding glass to use is one with a composition slightly amended from the core glass composition in a way that reduces the refractive index by a small fraction. However, this approach was not implemented in this research due to its very expensive cost of the large amounts of high grade GeO_2 raw materials required to make a modified lead-germanate cladding. Instead, the commercial Schott SF series lead-silicate glasses were considered as possible candidates for cladding materials because their optical, thermal, and chemical properties might be matched to our lead-germanate core-glass. Also, these glasses could be acquired with a guaranteed high optical quality together with detailed information on their optical, chemical and thermal properties.

The major difficulty in selecting a suitable clad from the lead-silicate glasses, which have such a fundamentally different composition to our core glass, is in matching the viscosities of the cladding and the core glasses at the fiber pulling temperature. At the same time the cladding glass must also possess the desirable refractive index, matched thermal expansion coefficient, etc. to the core glass. Matching the T_g and T_s between the clad and the core, as we had reported for the lead-silicate glass fibers,[19] is no longer relevant, because the core and the clad belong to two distinctively different glass systems and have different viscosity temperature dependencies. Although it is well known that the viscosity η varies with temperature T, according to the following Arrhenius-type expression,[20]

$$\eta=\eta_0 \exp\left(\frac{E}{RT}\right), \tag{2}$$

where η_0 is a temperature-independent constant and E is the activation energy. It has been found[21] that the activation energy E decreases with increasing temperature, which makes the use of Eq. (2) for the theoretical prediction of the fiber pulling temperature range (corresponding to the viscosity of about 10^5 P for the rod-in-tube technique[18]) extremely difficult. Therefore, the only accurate method for determining the fiber pulling temperature of the possible cladding glasses is to try the glasses experimentally using its glass rod in the fiber pulling furnace to define the fibering temperature range. Of the Schott glasses tried, SF16 and SF56 were both found to have a similar fibering temperature range to the core glass, at around 700 °C.

To finally assess the suitability of SF16 and SF56 as cladding glasses it was necessary to compare the thermal expansion coefficients and refractive indices to the lead-germanate core glass. The refractive index n_D and the thermal expansion coefficient α of the lead-germanate core glass were calculated using Gan's method[16] to be 1.804 and $118.8\times10^{-7}\,°C^{-1}$, respectively. The error in this type of calculation was about $\pm7\times10^{-3}$ for the refractive index and $\pm6\times10^{-7}\,°C^{-1}$ for thermal expansion coefficient. The refractive index of the core glass was measured experimentally by the prism coupling method,[22] and found to be 1.812 ± 0.005 in reasonable agreement with the calculated figure. An experimental value for thermal expansion coefficient, α, was not available. Comparing the refractive index and thermal-expansion coefficient of the core glass with those of the SF16 (n_D of 1.646 and α of $93\times10^{-7}\,°C^{-1}$) and the SF56 (n_D of 1.784 and α of $88\times10^{-7}\,°C^{-1}$), it was confirmed that both of these cladding glasses would provide a guiding structure for optical fibers and both cladding glasses also had well-matched thermal-expansion coefficients to that of the lead-germanate core glass [$\Delta\alpha<50\times10^{-7}\,°C^{-1}$ (Ref. 23)].

B. Fiber fabrication

The fiber fabrication was performed by the rod-in-tube technology.[19] The core and cladding were drilled out from the corresponding bulk glasses with an ultrasonic drilling machine. The ultrasonically cleaned lead-germanate core-glass rod (10 mm in diameter) was further caned into 1–2 mm in diameter in the fiber drawing furnace, with a hot zone of 20 mm in length $\times$20 mm in diameter, to ensure a fire polished smooth surface ready for use as the fiber core. The cladding-glass rod with an appropriate drilled hole area in the middle could either be priorly chemically polished using 5% HF solution for about 15–30 sec, or be used directly after thorough cleaning without chemical polishing to form the rod-in-tube combination. As shown in Fig. 1(c), the nonprior etched cladding was able to be fire polished in the hot zone of fiber pulling furnace just before the fiber was drawn at around 700 °C.

Figure 5 shows the cross section of optical fiber drawn with the combination of the optimized lead-germanate as core and the Schott SF56 lead-silicate as cladding by the rod-in-tube technique. A fine, clean, and well-defined core-clad interface can be clearly seen, showing good chemical compatibility between these two different types of glasses at the fiber pulling temperature range. The mechanical strength of the fibers was also good displaying a bending radius of 5 mm possible in uncoated fiber, which is comparable with the bending radius obtainable in bare silica fibers. Fibers have been pulled with 3–10 μm core diameters and more than 50 m in length, with either SF56 or SF16 as a cladding. The background fiber loss was typically 2 dB/m and probably represents the background loss

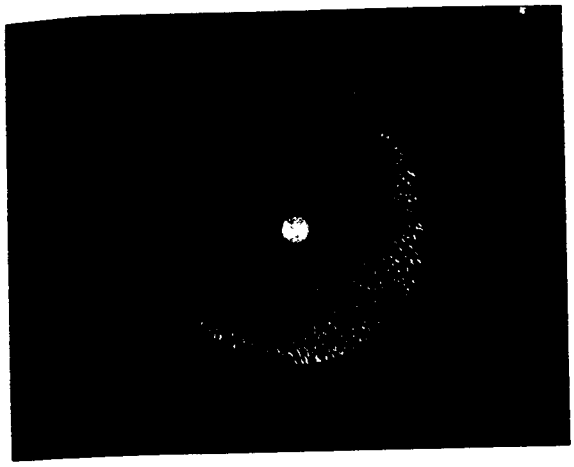

FIG. 5. Cross section of the fiber with GPBZK as core and Schott glass SF56 as cladding.

of the bulk glass used in the fiber core, which was limited by the purity of the starting materials or the manufactural conditions, with minimal losses therefore attributable to imperfections in the fiber.

V. SPECTROSCOPIC CHARACTERIZATION

A. Vibrational spectroscopy

Raman spectra of the bulk lead-germanate glass, $55GeO_2$-$20PbO$-$10BaO$-$10ZnO$-$5K_2O$:Tm_2O_3, used in the fiber core and an "in house" melted pure germanate glass are presented in the upper and lower halves of Fig. 6. Full Raman spectra from 200 to 1400 cm^{-1} are shown for 514.5 nm Ar^+-ion laser excitation and the insert shows the Raman spectra of the GPBZK glass above 600 cm^{-1} excited with the 488 nm Ar^+ line.

The Raman spectra of the pure GeO_2 agrees with similar results previously reported by Galeener and Lucovsky.[24] The spectra given in the upper half of Fig. 6 for the GPBZK given are complicated by the presence of erbium contamination in the GPBZK glass. The peaks in the 514.5 nm excited Raman spectra, marked with an asterisk in Fig. 6, can be attributed to erbium fluorescence on the Er^{3+} $^4S_{13/2}$–$^4I_{15/2}$ and Er^{3+} $^2H_{11/2}$–$^4I_{15/2}$ transitions. This is confirmed for the peak at over 1200 cm^{-1} (=550 nm) by its disappearance from the Raman spectra excited at 488 nm, out of resonance with the Er transition. However, a similar confirmation of the Raman peaks below 600 cm^{-1} was not possible, due to fluorescence from the $^1G_4$ level of the thulium doped into the glass dominating Raman scattering at frequencies below 600 cm^{-1}, relative to 488 nm. The source of the erbium contamination of the GPBZK glass was the original thulium oxide. Close examination of the white light absorption of bulk PKBZG glass revealed a very tiny absorption peak at around 550 nm corresponding to the strongest of the Er^{3+} absorption lines. A quantitative measure of the strength of this absorption was not possible, but its apparent size in relation to the thulium absorption leads us to suggest the erbium concentration is below 1 ppm.

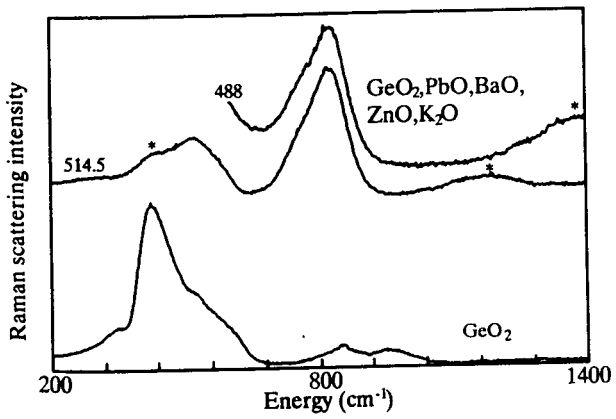

FIG. 6. Raman spectra of GPBZK and pure GeO_2 glasses, excited at 488 and 514.5 nm.

The Raman spectra of the other bulk lead germanates fabricated with compositions CaO-PbO-GeO_2 and CaO-PbO-Al_2O_3-GeO_2 were also recorded and appeared almost identical to the spectra given in the upper half of Fig. 6 for the GPBZK glass.

The drastic change in the Raman spectra from pure germanate (lower spectra, Fig. 6) to lead germanates (upper spectrum, Fig. 6), can be attributed to the effect of the lead on the GeO_2 glass structure. It has been postulated by Hagiwara and Oyamada[25] that PbO distorts, but does not destroy, the tetrahedral GeO_4 network in the lead-germanate glass. It is suggested that Pb^{2+} breaks some of the bridging bonds of the oxygen ions in the glass which join the Ge^{4+} ions. The very strong covalent nature of the lead with the oxygen distorting the GeO_4 tetrahedra and hence reducing the frequency of the antisymmetric stretching modes of the GeO_4 tetrahedra, by weakening the Ge—O bonds. If the highest-energy vibrational peaks observed in the Fig. 6 are attributed to these antisymmetric stretching vibrations then the observed shift to lower energy of these vibrations is consistent with the strong covalent interaction of the lead with the oxygen ions.

The particular interest in the vibrational spectra of these glasses is in the highest vibrational energy, because of its effect on nonradiative multiphonon decay of dopant rare-earth ions. The rate of nonradiative decay is very sensitive to the maximum vibrational energy of the glass.[26] The maximum vibrational energies for ZBLAN and aluminosilicate glasses are 580 and 1150 cm^{-1}, respectively.[27] From the spectra in Fig. 6, it can be seen that the energy of the highest Raman peak in pure germanate glass is 980 cm^{-1}, and that of lead-germanate glass is 820 cm^{-1}, intermediate between ZBLAN and silica glasses. The difference in the maximum vibrational energies of silica, ZBLAN, and lead-germanate glasses is enough to radically change the quantum efficiency of luminescence emission from dopant rare-earth ions. In particular, the quantum efficiencies of the $^3F_4$ and $^3H_4$ levels of thulium can be changed by use of a lead germanate host in such a way as to significantly enhance the performance of diode-pumped 2 μm lasers, as detailed in a later section.

We note that in these glasses, the highest-energy Ra-

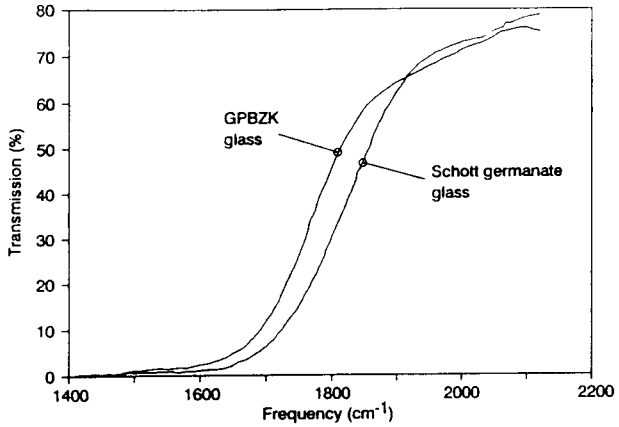

FIG. 7. Infrared transmission of GPBZK glass and a commercial Schott germanate glass.

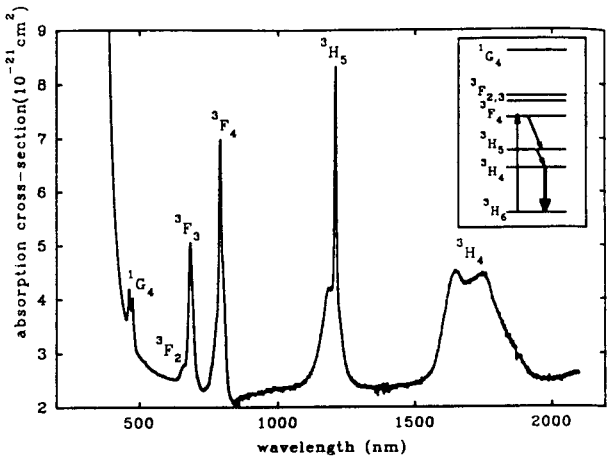

FIG. 9. Fluorescence lifetimes of (a) $^1G_4$, (b) $^3F_4$, and (c) $^3H_4$ levels of Tm^{3+} in different germanate-based glasses, showing the variation in lifetimes as composition is changed.

man peaks have a significant width. In order to make an accurate assessment of the nonradiative decay rates, it may be necessary to take some account of these widths.

B. Absorption

Figure 7 shows the infrared absorption edges of GPBZK glass and a commercial Schott germanate glass. From this figure it can be seen that the *ir* absorption edge is shifted to lower energy in the GPBZK glass. This is expected from the reduction in the maximum vibrational energy shown by the Raman spectra in Fig. 6. This increase in *ir* transparency is a particular bonus in the production of low-loss fibers in the 2 μm region.

The absorption cross section for 0.5 wt % doped GPBZK glass in presented in Fig. 8. Energy level assignments for the various thulium absorption bands are also given above the absorption peaks. Absorption data was recorded from a polished slab of bulk glass, taken from the same melt batch used to fabricate the final fiber core. The value of the absorption cross section was calculated from the white light absorption in dBm^{-1} using a glass density of 5.7 g/cm^3, measured by the Archimedes method, and a Tm_2O_3 concentration of 0.5 wt %, equivalent to 8.7×10^{19} ions cm^{-3}. The assignment of the energy levels; in particular, the $^3F_4$ and $^3H_4$ bands, follows the zero spin-orbit coupling convention.[28]

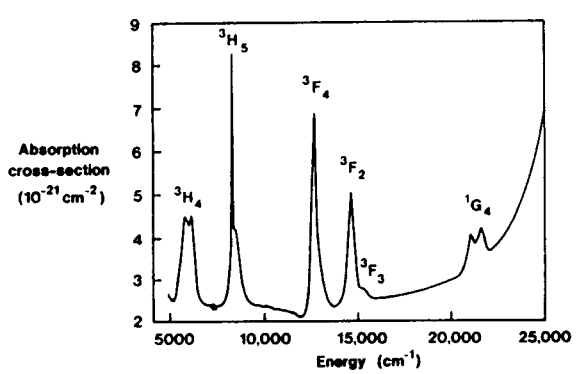

FIG. 8. Absorption spectrum of GPBZK glass. The insert shows the thulium energy level diagram, and highlights the 790 nm pumping scheme for 1.9 μm laser operation.

The positions of the absorption peaks, shown in Fig. 8, for the GPBZK glass are very similar to thulium doped fluorozirconate based glass, e.g., ZBLA,[29] and are therefore shifted slightly from thulium silicates.[30] The spectral width of the absorption bands for Tm^{3+} in PKBZG is intermediate between Tm^{3+} fluorozirconates and Tm^{3+} silicates. From the spectra it can seen that the absorption into both the $^3H_4$ and the $^1G_4$ levels has a double peak structure, unseen in either fluorozirconate based or silica based thulium hosts, indicating rather well-defined local environments around Tm^{3+} in the PKBZG glass.

C. Fluorescence decay

Given in Fig. 9 are the fluorescence decay lifetimes for the $^1G_4$, $^3F_4$, and $^3H_4$ levels of thulium doped into pure GeO_2, CaO-PbO-GeO_2, CaO-PbO-Al_2O_3-GeO_2 and 55GeO_2-20PbO-10BaO-10ZnO-5K_2O bulk glasses and the initial GPBZK fiber. The fluorescence decay from the $^1G_4$ level was well represented by a single exponential decay. Single exponentials did not fit as well to the $^3F_4$ fluorescence decays, but the results of these fits will be used here to give a reasonable estimation of the $^3F_4$ lifetime. Explanations for the nonexponential behavior of the $^3F_4$ fluorescence decay in thulium have been given previously by Lincoln *et al.*[30] The quality of the single exponential fits to the $^3H_4$ decays was harder to assess due to the smaller dynamic range of fluorescence decay recorded. The $^3H_4$ lifetime for CaO-PbO-Al_2O_3-GeO_2 was not recorded.

The values for all $^3H_4$ lifetimes given in Fig. 9 are all substantially longer than the 500 μs lifetime measured for thulium in alumino-silicates.[31] This reflects the substantial decrease in the maximum vibrational energies of germanate glasses compared to silicate glasses (as noted from the Raman spectra). The observed $^3H_4$ lifetime for the pure thulium germanate, given as 2.27 ms in Fig. 8, agrees well with the 3 ms decay time predicted by Reisfeld,

Boehm, and Spector.[32] From the lower part of Fig. 9, it can be clearly seen that in the thulium-doped modified lead germanates the $^3H_4$ Tm^{3+} lifetime has been further extended from the value in pure GeO_2 glass. This change in lifetime is consistent with the lowering of the maximum vibrational energy of the modified lead germanates in comparison to pure germanates, as noted above.

The final $^3H_4$ lifetime given in the lower part of Fig. 9 for GPBZK fiber shows a substantial shortening of the $^3H_4$ lifetime from bulk glass to fiber of 3.16 to 2.35 ms. The reasons for this drastic shortening in the lifetime are at present unclear. It is possible that this lifetime is quenched by energy transfer to defects in the glass, with a higher number of these present in the fiber. Similar lifetime shortening effects have also been seen for other thulium levels when comparing silica-based fibers and their preforms[30] and have been attributed to cross-relaxation mechanisms, which are more apparent in fibers because of the higher excitation intensities. The probability of cross relaxation occurring in the GPBZK glass is high due to the high thulium concentration of 8.7×10^{19} ions cm^{-3}. This concentration is equivalent to a Tm-ion separation of $\approx$22.5 Å (assuming a homogeneous dopant distribution). This ion separation is close to the critical ion separation for efficient energy transfer, reported to be around 20 Å.[33] Cross relaxation has also been recorded at Tm^{3+}-ion separations of 35 Å in fluorozirconate glasses,[29] although clustering of the thulium ions was suggested in these glasses. It is possible that the thulium ion distribution in the fiber is different from that in the bulk glass due to the much higher quenching rate occurring on fiber drawing. This could change the probability for cross relaxation by slightly modifying the mean thulium ion separation. It is also possible that the high light intensities in the fiber build up sufficient population inversion in the $^3H_4$ level for amplified spontaneous emission from the level to become significant and thus shorten the lifetime.

The mid part of Fig. 9 shows the change in Tm^{3+} $^3F_4$ lifetime between the various bulk germanates discussed previously and the final fiber. These $^3F_4$ lifetimes are all greater than the $^3F_4$ lifetime in silica-based fibers, where 20 μs has been reported.[30] A further lengthening of the $^3F_4$ lifetime is also observed from pure germanate to lead-germanate glasses, consistent with the shift in the maximum vibrational energy. For some applications, such as the diode pumped 2 μm thulium laser,[31] it is important that decay from the $^3F_4$ level does not become totally dominated by radiative processes to the ground state, since fast multiphonon emission from the $^3F_4$ level, via $^3H_5$ level to the upper laser level, $^3H_4$, is responsible for the high pump efficiency. Taking the Tm^{3+} $^3F_4$ radiative lifetime as falling within the range measured in other glasses, namely, 1.2–0.8 ms,[29,32] then the branching ratio for multiphonon emission from the $^3F_4$ can be estimated for GPBZK glass to be in the range 60%–80%.

Shortening of the $^3F_4$ lifetime from bulk GPBZK to fiber can be seen in the midpart of Fig. 9, though the effect is less pronounced than that observed for the $^3H_4$ level. This is because any cross-relaxation rate must be significantly faster than $(20\ \mu s)^{-1}$ to be observable.

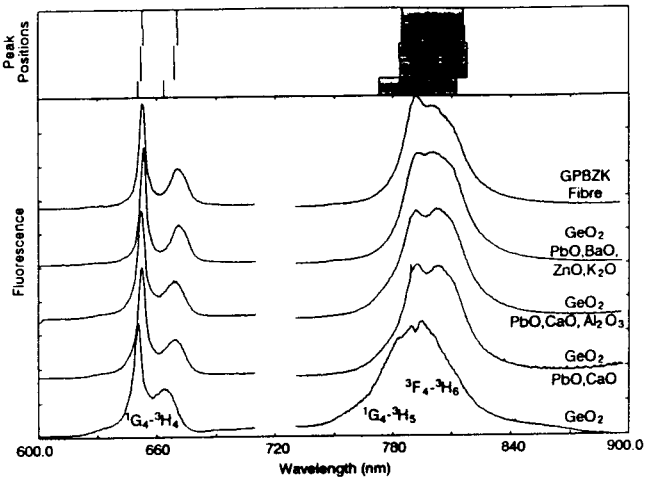

FIG. 10. Visible fluorescence spectra of Tm^{3+} in different GeO-based glasses. Changes in peak positions and fluorescence bandwidths are indicated in the top region of the figure.

The upper part of Fig. 9 shows the $^1G_4$ lifetimes for the germanate glasses discussed previously. The $^1G_4$ level is separated from the next lowest-lying energy level by an energy gap of >6000 cm^{-1}, making multiphonon emission from the $^1G_4$ level negligible even in silicate type glasses.[26] Therefore the observed lifetime of the $^1G_4$ level can be taken to be purely radiative for all glasses studied here, and comparisons of the $^1G_4$ lifetime between glasses can then be used to compare host dependent changes in the radiative decay process.

It was expected that the radiative lifetime of the germanates would be inversely proportional to the refractive index of the glasses through the refractive index factor in the Einstein A coefficient.[34] Between pure germanate and PbO-CaO-GeO_2 glass this is confirmed, with the $^1G_4$ lifetime reduced in the lead-germanate glass which has a much higher refractive index than pure germanate.[8] However, the $^1G_4$ lifetime for the other lead-germanate glasses is longer than pure germanate, as can be seen from the upper part of Fig. 9, despite the refractive index being higher in all the lead germanates, attaining a value of 1.812 in GPBZK glass. The reasons for this anomaly are unclear, especially since the major structural change in these germanate glasses occurs on the addition of lead rather than the other glass components. However, there may be other decay mechanisms, chiefly cross relaxation, which may be influencing the $^1G_4$ decay, independent of changes in the radiative rates.

D. Fluorescence spectra

Presented in Fig. 10 are the visible fluorescence spectra from 600 to 900 nm for all the thulium-doped glasses discussed previously (the upper and lower halves of each spectrum are scaled separately). The electronic transitions giving rise to each of fluorescence bands are also shown in Fig. 10. The insert above the spectra in Fig. 10 shows the

peak positions of the sharp fluorescence lines below 750 nm and a band is shown representing the full width at half maximum of the broad 790 nm peak.

Comparison of the fluorescence spectra for lead germanates with the fluorescence spectra for pure GeO_2, given as the lowest spectrum in Fig. 10 clearly shows a distinct narrowing and shift of the inhomogeneously broadened thulium spectrum in the lead germanates. The narrowing of the inhomogeneous profile indicates a smaller variation in the thulium site in the lead germanates, which reflects the more stable glass forming characteristics of the lead germanates.

Figure 10 shows that the change in the emission spectrum on adding lead to the germanate glass is much greater than any changes seen when adding further components to the lead germanate. This confirms the dominant effect of lead on the glass structure as was previously indicated by the Raman spectra. The visible fluorescence spectra for the various different thulium-doped lead-germanate compositions, shown in the mid part of Fig. 10, show very little change as additional glass components are added. In particular, no significant spectral shifts are observed on the addition of alumina. This is in distinct contrast to thulium-doped silica, in which large changes occur in the fluorescence properties of thulium-doped aluminosilicates when compared to pure silica or germanosilicate hosts.[30] As was discussed previously, in silica it is the alumina that acts to create a more stable glass giving the observed spectral shifts. In the case of the modified lead germanates it is clear that alumina has very little effect on the glass network. This echoes the conclusions of the thermal analyses of the bulk lead-germanate glasses discussed previously, where addition of alumina had little effect on the glass properties of the melt and agrees with the Raman spectra where no notable change was seen in the vibrational spectra on addition of alumina.

The slight peak narrowing observable in Fig. 10 between the fluorescence spectra for $CaO\text{-}PbO\text{-}GeO_2$ or $CaO\text{-}PbO\text{-}Al_2O_3\text{-}GeO_2$ and $PbO\text{-}K_2O_3\text{-}BaO\text{-}ZnO\text{-}GeO_2$ (GPBZK), indicates an even smaller variation of the thulium site in the GPBZK glass than other lead germanate. This is in accord with the excellent glass forming abilities of the GPBZK glass and supports the greater effect ZnO has on stabilizing the glass. No significant spectral changes are seen in the fiber when compared to the bulk GPBZK glass. The change in the form of the 790 nm peak in the fiber is attributed to a change in the proportions of $^3F_4$–$^3H_6$ and $^1G_4$–$^3H_5$ fluorescence making up this emission band due to much higher light intensities in the fiber.

The infrared emission spectra from 1.3 to 2.3 μm for the thulium-doped GPBZK glass fiber is presented in Fig. 11. Fluorescence from both the $^3H_4$–$^3H_6$ and $^3F_4$–$^3H_4$ transition is observed in the infrared spectrum. The fluorescence intensity of the $^3H_4$–$^3H_6$ transition shows less than a 6% variation over a 100 nm range at the peak of the emission. It should therefore be possible to achieve a large, flat tuning curve from a laser based on this transition.

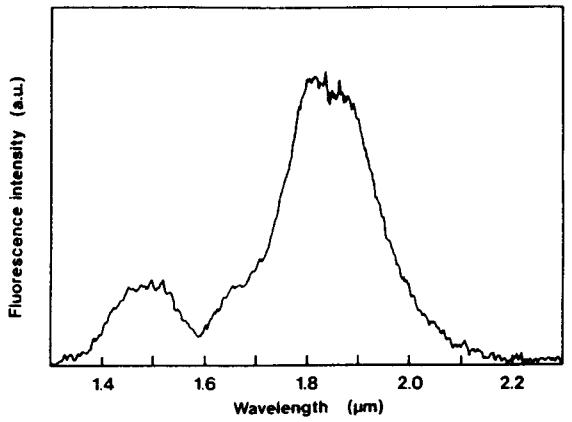

FIG. 11. Infrared emission spectrum of the transition from $^3H_4$–$^3H_6$ in Tm^{3+}:GPBZK fiber.

E. Lasing results

We have previously reported lasing results for the $^3H_4$–$^3H_6$ transition at around 1.9 μm in the GPBZK fiber.[6] The minimum reported threshold was 3.6 mW of launched light from 790 nm diode using just 3 cm of fiber. This compares to thresholds of 50 mW in ZBLAN[35] and 4.4 mW in alumina silica.[30] The best slope efficiency of the GPBZK laser was 13% from a cavity utilizing Fresnel reflection from a bare fiber end to provide lasing feedback and act as a 90% output coupler. The best slope efficiency for silica fiber has been reported as 17% and 8.3% has been reported for Tm^{3+}:ZBLAN fiber (simultaneously lasing at 1.48 μm). The lasing results for Tm^{3+}:GPBZK fiber therefore demonstrate considerable gains in threshold over previous demonstrations of lasing on the Tm^{3+} $^3H_4$–$^3H_6$ transition. Further improvements are anticipated with the optimization of the fiber length used in the fiber cavities.

VI. CONCLUSION

We have presented a study of a new class of optical fibers based on lead-germanate glass. These fibers provide an important new host for rare-earth ion based active devices, because of their vibrational energy, which lies between the vibrational energies of the two common optical fiber hosts, silica and ZBLAN. This enables the use of changes in radiative and nonradiative decay rates to engineer the development of a particular device. The rare-earth system we have studied is thulium, whose level structure is such that the balance between nonradiative and radiative decay is critical for the production of a useful laser operating at 2 μm. We have showed that the spectroscopic and vibrational properties of this glass host are ideal for the production of such a device. Fabrication of fibers has been successfully achieved by modification of the glass host by use of the Levin–Block concept. This novel use of the Levin–Block concept has allowed us to retain the valuable optical and vibrational properties of the glass while also achieving excellent thermal stability for fiber fabrication. The end result is a low-loss high-strength fiber which is ideal for many applications in active fiber devices.

[1] P. Urquhart, IEE Proc. Pt. J **135**, 385 (1988).
[2] E. M. Levin and S. Block, J. Am. Ceram. Soc. **40**, 95, 113 (1957).
[3] E. M. Levin and S. Block, J. Am. Ceram. Soc. **41**, 49 (1958).
[4] E. M. Levin and S. Block, J. Am. Ceram. Soc. **50**, 29 (1967).
[5] A. Tropper, R. Smart, I. Perry, D. Hanna, J. R. Lincoln, and W. S. Brocklesby, Proc. SPIE **1373**, 152 (1990).
[6] J. R. Lincoln, C. J. Mackechnie, J. Wang, W. S. Brocklesby, R. S. Deol, A. Pearson, D. C. Hanna, and D. N. Payne, Electron. Lett. **11**, 1021 (1992).
[7] W. H. Dumbaugh, Proc. SPIE **297**, 80 (1981).
[8] W. H. Dumbaugh, Opt. Eng. **24**, 257 (1985).
[9] D. L. Wood, K. Nassau, and D. L. Chadwick, Appl. Opt. **21**, 4276 (1982).
[10] A. F. Fray and S. Nielsen, Infrared Phys. **1**, 175 (1961).
[11] J. Zarzycki, *Glasses and the Vitreous State* (Cambridge University, Cambridge, England, 1991), p. 68.
[12] N. J. Kreidl, in *Glass Science and Technology*, edited by D. R. Uhlmann and N. J. Kreidl (Academic, New York, 1983), Vol. 1, Chap. 3, p. 183.
[13] E. M. Levin, in *Phase Diagram: Material Science and Technology*, edited by A. M. Alper (Academic, New York, 1970), Vol. 3, p. 144.
[14] J. Zarzycki, *Glasses and Vitreous State* (Cambridge University, Cambridge, England, 1991), p. 155.
[15] W. Eitel, *Silicate Science*, Vol. 2 (Academic, New York, 1965), p. 206.
[16] F. X. Gan, *Calculation of Physical Properties and Composition Design for Inorganic Glasses* (Shanghai Science, Shanghai, 1981).
[17] B. Phillips and M. G. Schroger, J. Am. Ceram. Soc. **48**, 398 (1965).
[18] W. Eitel, *Silicate Science* (Academic, New York, 1976), Vol. 7, p. 21.
[19] E. R. Taylor, D. J. Taylor, L. Li, M. Tachibana, J. E. Townsend, J. Wang, P. J. Wells, L. Reekie, P. R. Morkel, and D. N. Payne, Mater. Res. Soc. Symp. Proc. **172**, 321 (1990).
[20] N. P. Bansal and R. H. Doremus, *Handbook of Glass Properties* (Academic, New York, 1986), p. 223–227.
[21] A. Paul, *Chemistry of Glasses* (Chapman and Hall Ltd., London, 1982), pp. 76–85.
[22] J. H. Dickson, *Optical Instruments and Techniques* (Oriel, London, 1969).
[23] G. Orcel, D. Biswas, M. R. Shahriari, T. Iqbal, and G. H. Siegel, in *Proceedings of the 6th International Symposium Halide Glasses*, edited by G. H. Frischat (Clausthal-Zellerfeld, Federal Republic of Germany, 1989), p. 539-544.
[24] F. L. Galeener and G. Lucovsky, Phys. Rev. Lett. **37**, 1474 (1976).
[25] H. Hagiwara and R. Oyamada, J. Phys Soc. Jpn. **36**, 517 (1974).
[26] C. B. Layne, W. H. Lowdermilk, and M. J. Weber, Phys. Rev. B **16**, 10 (1977).
[27] B. Bendow, P. K. Bannerjee, M. G. Drexhage, J. Goltman, S. S. Mitra, and C. T. Moynihan, J. Am. Ceram. Soc. **65**, C8 (1982); S. G. Kosinski, D. M. Krol, T. M. Duncan, D. C. Douglass, J. B. MacChesney, and J. R. Simpson, J. Non-Cryst. Solids **105**, 45 (1988).
[28] S. Hufner, *Optical Spectra of Transparent Rare Earth Compounds* (Academic, New York, 1978).
[29] E. W. J. l. Oomen, J. Lumin. **50**, 317 (1992).
[30] J. R. Lincoln, W. S. Brocklesby, F. Cusso, J. E. Townsend, A. C. Tropper, and A. Pearson, J. Lumin. **50**, 297 (1991).
[31] W. L. Barnes, J. E. Townsend, and J. R. Lincoln, Electron. Lett. **26**, 746 (1990).
[32] R. Reisfeld, L. Boehm, and N. Spector, Chem. Phys. Lett. **49**, 251 (1977).
[33] G. Blasse, in *Spectroscopy of Solid State Laser-Type Materials*, edited by B. DiBartolo (Plenum, New York, 1987), p. 199.
[34] W. M. Yen, *Laser Spectroscopy of Solids*, edited by W. M. Yen and P. M. Selzer (Springer, Berlin, 1981), p. 3.
[35] J. N. Carter, Ph.D thesis, Southampton University, 1992 (unpublished).